



Cite this: RSC Adv., 2025, 15, 47383

# Comprehensive review of *Bletilla striata* polysaccharides: from fundamental studies to innovative biomaterials

Jinxiang Fu,<sup>†a</sup> Yi Lu,<sup>†b</sup> Wennuo Xu,<sup>a</sup> Kangdi Hu,<sup>a</sup> Ting Cao,<sup>a</sup> Ronghua Fan<sup>\*ac</sup> and Song Cang<sup>id\*<sup>a</sup></sup>

*Bletilla striata* (Thunb.) Rchb.f. is a perennial medicinal orchid with a well-documented history in traditional Chinese medicine spanning millennia. Clinically employed for treating mucosal injuries, ulcers, trauma, and burns, this botanical exhibits diverse pharmacological properties attributed to its rich composition of bioactive compounds. Among these constituents, *Bletilla striata* polysaccharides have emerged as the primary pharmacologically active components, demonstrating remarkable anti-inflammatory activity, wound healing, hemostatic activity, antioxidant activity, and antimicrobial activity. When compounded with macromolecular components to create emerging hydrogels, sponges, microneedles, eye drops and films, the resulting materials surpass traditional products in mechanical performance, biocompatibility and biodegradability, offering an ideal platform for wound management, tissue repair and regenerative medicine. Future clinical translation of BSPs will be advanced by optimizing scalable production and systematically evaluating the clinical safety of its biomaterials. In this paper, the research progress of extraction and purification, chemical structure characterization, biological activity of BSPs and new BSP-based composite biomaterials that harness the biological activity of BSP in recent years were reviewed. This paper will promote the understanding of BSP and provide a theoretical basis for the development of new biological materials.

Received 9th September 2025  
Accepted 19th November 2025

DOI: 10.1039/d5ra06806a

rsc.li/rsc-advances

## 1. Introduction

The genus *Bletilla* Rchb.f. (Orchidaceae) represents a group of perennial herbaceous plants comprising approximately six recognized species, predominantly distributed across East Asia, including northern Myanmar, China, South Korea, and Japan.<sup>1</sup> Within the Chinese territory, four distinct species have been identified and characterized: *B. formosana* (Hayata) Schltr., *B. ochracea* Schltr., *B. sinensis* (Rolfe) Schltr., and *B. striata* (Thunb.) Rchb.f. (Fig. 1 and Table 1).<sup>2</sup> Among these species, *Bletilla striata* has emerged as the most pharmacologically significant, characterized by its robust erect stems (12–60 cm in height), 4–6 lanceolate leaves, and distinctive purple to lavender inflorescences, giving it both ornamental and medicinal value.

Traditional Chinese Medicine (TCM) classifies *B. striata* as a herb with a bitter taste, neutral thermal nature, and non-toxic properties. Its therapeutic applications have been well-documented in classical medical texts for the treatment of

various conditions, including but not limited to epistaxis, hematemesis, pulmonary injuries, gastrointestinal hemorrhage, and dermatological disorders.<sup>3</sup> Contemporary pharmacological studies have substantiated these traditional uses through the identification of multiple bioactive properties, including immunomodulatory,<sup>4</sup> antioxidant effects,<sup>5</sup> anti-inflammatory effects,<sup>6</sup> antibacterial effects,<sup>7</sup> hemostatic,<sup>8</sup> anti-influenza virus,<sup>9</sup> anti-cancer<sup>10</sup> and other activities.<sup>11,12</sup>

The tuberous roots of *B. striata* constitute the primary medicinal component, containing a complex array of bioactive compounds. Recent phytochemical investigations have identified hundreds of constituents, including polysaccharides (approximately 30% of dry weight),<sup>13</sup> phenanthrenes and their derivatives, dihydrophenanthrenes, and biphenyl compounds.<sup>14</sup> Among these, *Bletilla* polysaccharides (BSPs) have garnered particular attention due to their demonstrated pharmacological efficacy, particularly in anti-inflammatory, antioxidant, antimicrobial, and hemostatic applications.<sup>14</sup> The structural complexity and biological activities of BSPs have positioned them as promising candidates for the development of novel therapeutic agents and biomaterials.

The burgeoning interest in plant-derived polysaccharides as innovative biomaterials has gained substantial momentum in recent years, driven by their biocompatibility, biodegradability, and versatile biological activities.<sup>15,16</sup> While numerous studies have extensively documented the pharmacological profile of

<sup>a</sup>Department of Sanitary Inspection, School of Public Health, Shenyang Medical College, No. 146, North Huanghe Street, Shenyang 110034, Liaoning province, China. E-mail: cangsong517@163.com; ronghuafan1@126.com

<sup>b</sup>Second Affiliated Hospital of Shenyang Medical College, Shenyang 110032, China

<sup>c</sup>Shenyang Key Laboratory of Chronic Disease Assessment and Nutritional Intervention for Heart and Brain, Shenyang Medical College, Shenyang 110034, China

<sup>†</sup> Jinxiang Fu and Yi Lu contributed equally to this work.



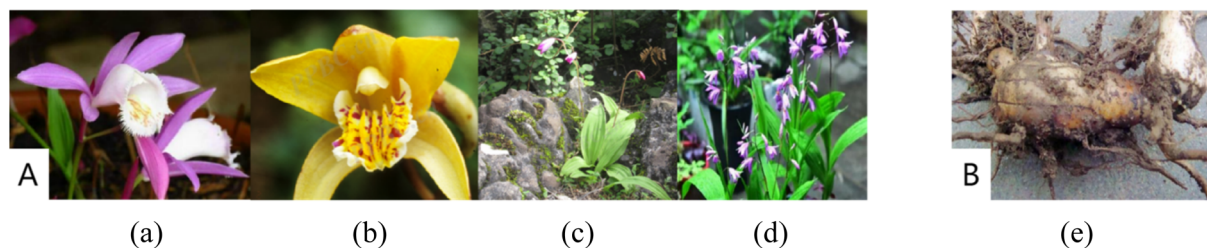


Fig. 1 (A) Four kinds of *Bletilla* flowers: *Bletilla formosana* (a), *Bletilla ochracea* (b), *Bletilla sinensis* (c), *Bletilla striata* (d) (B) *Bletilla* tubers (e). (pictures from 'Flora of China' and WeChat public number: Changyang Hospital of Traditional Chinese Medicine).

Table 1 Distribution of *Bletilla* Rchb.f

Latin name	Chinese name	Distribution
<i>Bletilla formosana</i>	"Xiao Bai Ji" (小白及)	China
<i>Bletilla ochracea</i>	"Huang Hua Bai Ji" (黄花白及)	China
<i>Bletilla sinensis</i>	"Hua Bai Ji" (华白及)	China
<i>Bletilla striata</i>	"Bai Ji" (白及)	China, Japan, South Korea
<i>Bletilla guizhouensis</i>	"Gui Zhou Bai Ji" (贵州白及)	China
<i>Bletilla chartacea</i>	"Mian Dian Bai Ji" (缅甸白及)	Northern Myanmar

BSPs,<sup>17,18</sup> the exploration of their potential as functional biomaterials remains relatively unexplored. This paper aims to review the application potential of its biomaterials in biomedicine based on the biological activity of BSP, and summarize the extraction process and structural characteristics of BSP, so as to provide reference for further development of BSP biomaterials and promote the application and development of BSP in the future.

## 2. Structural characteristics of polysaccharides from *Bletilla striata*

The chemical structure of polysaccharides is often closely related to their biological activity and pharmacological effects. It is necessary to study and describe the biological activity of polysaccharides and understand their structural characteristics. At present, more and more biological activities of *Bletilla striata* polysaccharide have been found, and its structural characteristics have also been paid attention to by many scholars. The main structural characteristics include its molecular weight, monosaccharide composition, chemical structure and glycosidic bond position. Common structural characterization methods include high performance gel permeation chromatography, high performance liquid chromatography, infrared spectroscopy, nuclear magnetic resonance, gas chromatography and mass spectrometry or a combination of the two, Fourier transform infrared spectroscopy, methylation analysis, acid hydrolysis and other analytical methods.

### 2.1. Molecular weight

The molecular weight distribution of BSPs is typically characterized using two primary parameters: number-average molecular weight ( $M_n$ ) and weight-average molecular weight ( $M_w$ ), with  $M_w$  being more commonly reported due to its greater

relevance to solution properties and biological activities. Size-dependent separation techniques, particularly high-performance gel permeation chromatography (HPGPC),<sup>19</sup> have emerged as the gold standard for molecular weight determination of BSPs. HPGPC operates on the principle of size exclusion chromatography (SEC), where polysaccharide molecules are separated based on their hydrodynamic volume through porous stationary phases with defined pore size distributions. This technique offers several advantages, including non-destructive analysis, high reproducibility, and compatibility with various detection systems such as refractive index (RI) and multi-angle laser light scattering (MALLS) detectors.

The molecular weight profile of BSPs exhibits significant variation depending on extraction methodologies. Comparative studies have demonstrated that conventional hot water extraction typically yields BSPs with higher molecular weights (282.91–402.17 kDa),<sup>5</sup> while alkaline extraction and ultrasonic-assisted methods tend to produce lower molecular weight fractions (195.83–230.63 kDa).<sup>5,20</sup> Recent investigations have further elucidated this molecular weight diversity, with reported values ranging from 10 kDa to 500 kDa across different extraction protocols and purification fractions (Table 2). Specifically, alkaline-extracted BSP fractions have shown a broad molecular weight distribution (28.153–269.121 kDa),<sup>19</sup> while hot water-extracted BSPs generally maintain higher molecular weights (229–255.172 kDa).<sup>21,22</sup> Notably, gel permeation chromatography (GPC) analyses have identified low molecular weight BSP fractions (28 365 Da),<sup>23</sup> suggesting the presence of oligosaccharide components in certain preparations.

### 2.2. Monosaccharide composition

Polysaccharides are complex biopolymers composed of monosaccharide units linked through glycosidic bonds, which can be



Table 2 Structural characteristics and extraction methods of *Bletilla striata* polysaccharides

Name	Monosaccharide composition (% molar ratio)	Molecular weight ( $M_w$ )	Structural characteristics	Extraction method	Ref.
BSPb	Glu : Man = 1 : 3	$2.60 \times 10^5$ Da	The main chain formed by (1 $\rightarrow$ 2) and (1 $\rightarrow$ 4) glycosidic bonds	Hot water extraction	27
pFSP	D-Glu : D-Man : D-Galactose = 1 : 2.03 : 3.45	$9.10 \times 10^4$ Da	The main chains of (1 $\rightarrow$ 4)-connected $\alpha$ -D-Glcp, (1 $\rightarrow$ 4)-connected $\beta$ -D-Manp and (1 $\rightarrow$ 3, 6)-connected $\beta$ -D-Manp units	Hot water extraction	24
BSP	Man : Glc = 2.4 : 1.0	$1.35 \times 10^5$ Da	Backbone composed of 1,4-linked manp	Hot water extraction	28
BSP-1	Man : Glu = 4 : 1	$8.35 \times 10^4$ Da	The main chain is composed of $\beta$ -1,4-D-mannose and $\beta$ -1,4-D-glucose	Hot water extraction	40
BSP-2	Man : Glu = 3 : 1	$1.26 \times 10^4$ Da	The main chain is composed of $\beta$ -1,4-D-mannose and $\beta$ -1,4-D-glucose	Hot water extraction	40
BSP	Man : Glu = 2.946 : 1	$3.73 \times 10^5$ Da	A branched polysaccharide composed of (1 $\rightarrow$ 4)- $\beta$ -D-mannopyranose in the main chain	Hot water extraction	41
BSPF2	Man : Glu : Galactose = 9.4 : 2.6 : 1.0	$2.35 \times 10^5$ Da	The main chain is composed of (1 $\rightarrow$ 4)-mannose and (1 $\rightarrow$ 4)-glucose	Hot water extraction	25
BSP	Man : Glc = 7.45 : 2.55	$1.70 \times 10^5$ Da	—	Hot water extraction	42
BSP	Man : Glu = 2.9 : 1	$2.80 \times 10^4$ Da	The main chain is (1 $\rightarrow$ 6)- $\beta$ -Manp-(1 $\rightarrow$ , $\rightarrow$ 4)- $\beta$ -Glcp-(1 $\rightarrow$ , $\rightarrow$ 4)- $\beta$ -Manp (1 $\rightarrow$ , $\rightarrow$ 3)- $\alpha$ -Manp-(1 $\rightarrow$ ), $\beta$ -Glcp-(1 $\rightarrow$ and $\beta$ -Manp-(1 $\rightarrow$ ))	Hot water extraction	23
BSAP	Glu : Xylose : Man = 2.39 : 1.00 : 0.21	$2.29 \times 10^5$ Da	—	Hot water extraction	21
BSP	Man : Glu = 2.4 : 1	$1.46 \times 10^5$ Da	—	—	43
BSP-1	Galactose : Glu : Man = 0.53 : 24.91 : 74.56	$2.69 \times 10^5$ Da	The main chain is composed of $\alpha$ -D-Glcp, $\beta$ -D-Glcp, $\beta$ -D-Manp and 2-O-acetyl- $\beta$ -D-Manp	Alkali water extraction	20
BSP	Man : Glc = 3.5 : 1.0	$2.00 \times 10^4$ Da	Backbone composed of (1 $\rightarrow$ 4)-linked $\beta$ -D-glucopyranosyl residues and (1 $\rightarrow$ 4)-linked $\beta$ -D-mannopyranosyl residues	Ultrasonic-assisted extraction	44
LMW-BSP	Man : Glu = 1.26 : 1	$2.30 \times 10^4$ Da	The main chain is composed of $\alpha$ -D-manp-(1 $\rightarrow$ 3)- $\beta$ -D-manp-(1 $\rightarrow$ 4)- $\beta$ -D-Glcp-(1,2 $\rightarrow$ 4)- $\beta$ -D-manp-(1 $\rightarrow$ 3)- $\beta$ -D-manp-(1 $\rightarrow$ )	Water extraction	45
BVPS	Man : Glc = 7.37 : 2.63	$1.47 \times 10^5$ Da	—	Hot water extraction	46
BFPS	Man : Glc = 7.4 : 2.6	$9.55 \times 10^4$ Da	—	Hot water extraction	46
RBP	Man : Glc = 2 : 1	$8.20 \times 10^5$ Da	Backbone composed of $\beta$ -1,4-linked D-mannosyl residues and $\beta$ -1,4-linked D-glucosyl residues	Hot water extraction	47

classified as either homopolysaccharides (consisting of a single type of monosaccharide) or heteropolysaccharides (comprising multiple monosaccharide types). Structural analyses have revealed that BSPs predominantly exist as heteropolysaccharides, with glucose (Glc), mannose (Man), and galactose (Gal) constituting the primary monosaccharide components, although homopolysaccharide fractions have also been identified.

The monosaccharide composition of BSPs is typically determined using advanced chromatographic techniques, with ion chromatography (IC) and gas chromatography (GC) being the most widely employed methods. These techniques provide precise quantification of monosaccharide constituents and their molar ratios. For instance, ion chromatographic analysis of hot water-extracted pFSP revealed a molar ratio of D-Glc : D-Gal : D-Man = 1.00 : 2.03 : 3.45, indicating a mannose-rich polysaccharide structure.<sup>24</sup> Similarly, Liu *et al.*<sup>21</sup> identified Glc, Xyl, and Man in BSAP with a molar ratio of 2.39 : 1.00 : 0.21,

demonstrating the presence of xylose (Xyl) in certain BSP fractions. Gas chromatographic analysis of hot water-extracted BSPF2 further confirmed the heterogeneity of BSPs, showing a Man : Glc : Gal ratio of 9.4 : 2.6 : 1.0,<sup>25</sup> which suggests significant structural variability among different BSP fractions.

### 2.3. Chemical structure and glycosidic bond

Structural elucidation studies have identified BSPs as glucomannans characterized by a backbone predominantly composed of (1  $\rightarrow$  4)-linked  $\beta$ -D-mannopyranosyl and (1  $\rightarrow$  4)-linked  $\beta$ -D-glucopyranosyl residues (Fig. 2). Advanced structural characterization techniques, including methylation analysis, nuclear magnetic resonance (NMR) spectroscopy, and mass spectrometry-chromatography integration, have been instrumental in deciphering the complex architecture of BSPs.<sup>26</sup>

Comprehensive structural analyses have revealed significant heterogeneity in BSP configurations. Wang *et al.*<sup>27</sup> demonstrated through methylation and NMR analysis that BSPb

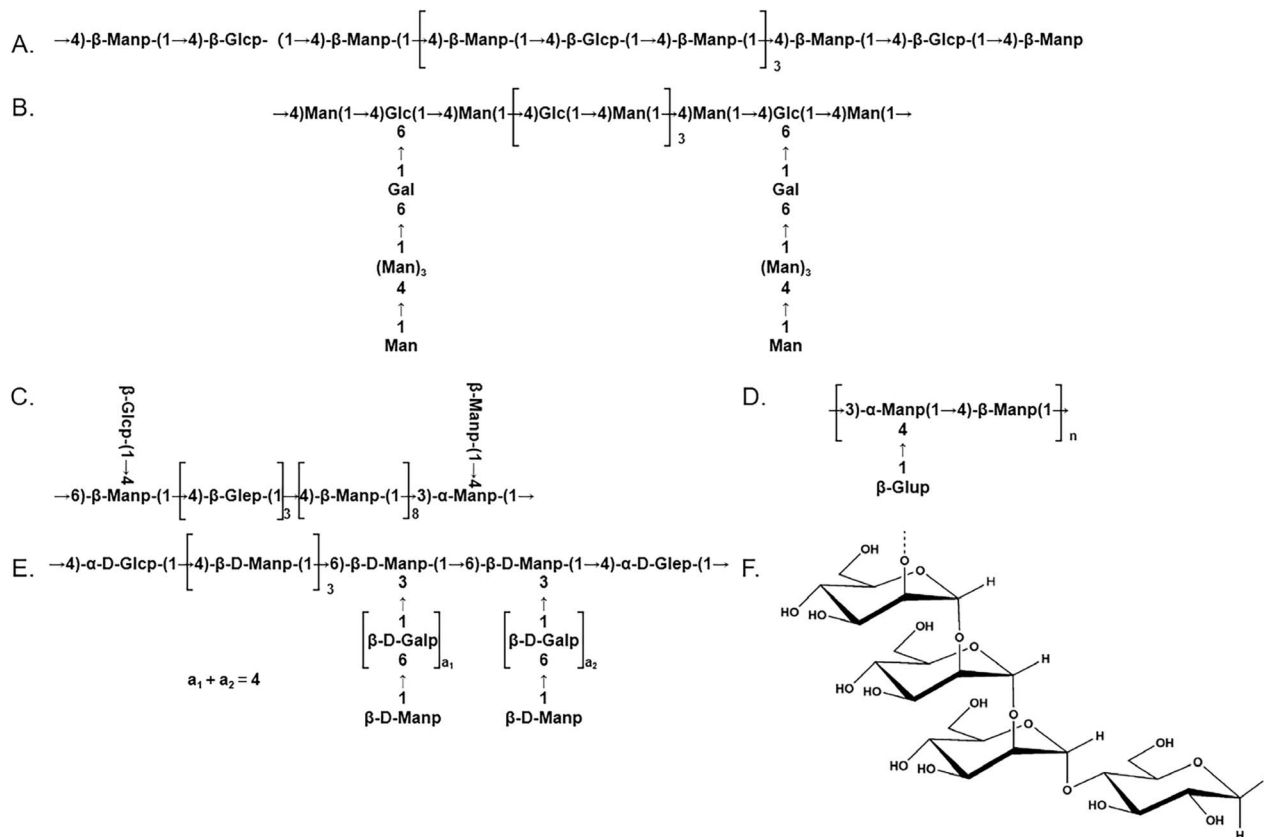


Fig. 2 The possible structural features of BSPs. (A) the structure of BSP-A/B/H/U;<sup>5</sup> (B) the structure of BSPF2;<sup>25</sup> (C) the structure of BSP;<sup>23</sup> (D) the structure of BSP;<sup>28</sup> (E) the structure of pFSP;<sup>24</sup> (F) the structure of BSPb.<sup>27</sup>

possesses a backbone structure primarily consisting of (1 → 2)-linked  $\alpha$ -D-mannopyranose and (1 → 4)-linked  $\beta$ -D-glucopyranose residues. Further structural investigations by Chen *et al.*<sup>20</sup> utilizing ion chromatography, gas chromatography-mass spectrometry (GC-MS), and NMR spectroscopy identified BSP-1 as containing  $\alpha$ -D-Glcp,  $\beta$ -D-Glcp,  $\beta$ -D-Manp, and 2-O-acetyl- $\beta$ -D-Manp residues, with branching units of  $\beta$ -D-Galp and  $\alpha$ -D-Glcp.

Notably, Qiu *et al.*<sup>22</sup> provided evidence of a triple-helical configuration in pBSP1 through Congo red binding assays, with NMR analysis revealing a glucose : mannose ratio of 1 : 2.95 and the presence of diverse glycosidic linkages, including (1 → 6), (1 → 2), and (1 → 4) bonds. Additional structural insights were provided by the identification of repeating units in hot water-extracted pFSP, which contained (1 → 4)- $\alpha$ -D-Glcp, (1 → 4)- $\beta$ -D-Manp, and (1 → 3,6)- $\beta$ -D-Manp units, with side chains terminated by (1 → )- $\beta$ -D-Manp residues.<sup>24</sup>

### 3. Extraction and purification method of *Bletilla striata* polysaccharide

#### 3.1. Extraction methods

The optimization of extraction protocols is crucial for obtaining BSPs with consistent structural integrity and biological activity. Current extraction techniques can be broadly classified into conventional methods and advanced assisted-extraction

technologies, each with distinct advantages in terms of yield, purity, and preservation of structural features. Table 2 summarizes the structural characteristics and extraction methods of BSPs.

**3.1.1. Hot water extraction methods.** The hot water extraction method, based on the hydrophilic properties of polysaccharides, enhances extraction efficiency through optimization of key parameters including extraction temperature, duration, and solid-liquid ratio. As the most established technique for BSP isolation, this method has been extensively studied using statistical optimization approaches such as response surface methodology (RSM) and orthogonal experimental design. Chen *et al.*<sup>5</sup> demonstrated that optimal extraction conditions (solid-liquid ratio of 1 : 30, extraction temperature of 70 °C, and duration of 3 hours) yielded a BSP extraction rate of 21.64%. While this traditional method offers advantages in terms of simplicity and scalability, it is associated with several limitations, including prolonged extraction times and significant energy consumption due to sustained heating requirements.

**3.1.2. Alkaline water extractions.** The alkaline water extraction method capitalizes on the enhanced solubility of polysaccharides under basic conditions, where partial cleavage of glycosidic bonds facilitates the release of polysaccharide components from the cellular matrix. This method shares the fundamental principle of water solubility with hot water





extraction but operates through an additional mechanism of alkaline-induced structural modification.<sup>29</sup> Optimization studies have demonstrated the effectiveness of this approach. Chen *et al.*<sup>5</sup> achieved an extraction yield of 18.29% using 0.005 mol per L NaOH at 60 °C for 3 hours. Further optimization by subsequent researchers established that extraction at 52 °C for 167 minutes with 0.01 mol per L NaOH could increase the yield to 29.53%.<sup>30</sup> While the alkaline extraction method generally provides higher extraction efficiency compared to conventional hot water extraction, it presents several limitations: (1) potential degradation of polysaccharide structure due to alkaline hydrolysis, (2) environmental concerns associated with alkali usage and waste disposal, and (3) possible alteration of bioactivity due to structural modifications.

**3.1.3. Enzymatic hydrolysis methods.** The enzymatic-assisted extraction method utilizes the catalytic activity of specific enzymes (*e.g.*, pectinases, cellulases) to degrade plant cell wall components, thereby enhancing the release and recovery of polysaccharides. This approach is particularly effective for disrupting the structural integrity of plant cells while preserving the target compounds' bioactivity.<sup>31</sup> Han *et al.*<sup>32</sup> demonstrated the efficacy of cellulase in BSP extraction, achieving a yield of 28.72% under optimized conditions: cellulase dosage of 17 600 U g<sup>-1</sup>, extraction temperature of 65 °C, and hydrolysis duration of 90 minutes. Further optimization by Sun *et al.*<sup>33</sup> using papain revealed that the highest polysaccharide purity (92%) could be achieved under the following conditions: extraction time of 120–150 minutes, pH 7.0–7.5, temperature of 45–50 °C, and enzyme dosage of 8–10 mg g<sup>-1</sup>. Compared to traditional extraction methods, enzymatic-assisted extraction offers several advantages: (1) higher extraction efficiency, (2) reduced environmental impact due to lower energy consumption and chemical usage, and (3) improved preservation of polysaccharide structure and bioactivity. However, this method is subject to strict reaction conditions, including precise control of pH, temperature, and enzyme activity, which may limit its scalability and industrial application.

**3.1.4. Ultrasonic extractions.** The ultrasonic-assisted extraction method leverages the physical cavitation effect of ultrasound waves to disrupt plant cell walls, facilitating the release of intracellular polysaccharides and enhancing solvent penetration. This non-thermal extraction technique significantly improves mass transfer efficiency through mechanical and thermal effects generated by ultrasonic waves.<sup>34</sup> Qiu *et al.*<sup>22</sup> employed an integrated optimization approach combining orthogonal design, Box–Behnken design (BBD), and genetic algorithm-back propagation (GA-BP) neural network modeling to determine the optimal extraction conditions for BSP. The optimized parameters (liquid-to-material ratio of 15 mL g<sup>-1</sup>, ultrasonic power of 450 W, and extraction time of 34 minutes) yielded a polysaccharide extraction rate of 8.29%, with notable antioxidant activity (26.20 ± 0.28 mM FE per mg). In a separate study, Han *et al.*<sup>32</sup> achieved a higher extraction yield (35.01%) for BSP-V under the following conditions: extraction time of 1 hour, ultrasonic power of 250 W, temperature of 30 °C, and liquid-to-solid ratio of 30 mL g<sup>-1</sup>. Compared to conventional

extraction methods, ultrasonic-assisted extraction offers several advantages: (1) significantly reduced extraction time, (2) improved extraction efficiency, and (3) lower energy consumption. However, the method's efficacy is highly dependent on optimal parameter control, including ultrasonic power, frequency, and extraction duration.

**3.1.5. Microwave extraction methods.** The microwave-assisted extraction method operates through two primary mechanisms: (1) the thermal effect, which induces rapid heating of polar molecules, and (2) the non-thermal effect, which enhances mass transfer by disrupting hydrogen bonds and dipole rotations. This technique facilitates the rapid transfer of target compounds from the plant matrix to the solvent by generating localized increases in temperature and pressure, thereby improving extraction efficiency.<sup>35</sup> Han *et al.*<sup>32</sup> optimized the microwave extraction of BSP-M, achieving an extraction yield of 42.82% under the following conditions: pH 7.0, solid–liquid ratio of 1 : 30, microwave power of 600 W, and extraction time of 9 minutes. This method demonstrates significant advantages over traditional techniques, including (1) higher extraction efficiency, (2) reduced solvent consumption, (3) shorter processing times, and (4) lower energy requirements. However, its application is limited by the high cost of specialized equipment and challenges in scaling up for industrial production.

**3.1.6. Infrared-assisted extraction methods.** As an emerging extraction technology, infrared-assisted extraction has gained attention for its ability to efficiently isolate bioactive compounds from plant materials. The method operates on the principle of infrared radiation-induced thermal effects, which enhance molecular vibration and thermal motion of polysaccharides within plant cells, thereby improving their solubility and mass transfer rates.<sup>36</sup> Qu *et al.*<sup>37</sup> pioneered the application of this technique for *Bletilla striata* polysaccharide extraction. Using a Box–Behnken design combined with response surface methodology, they optimized the extraction parameters and achieved a crude polysaccharide yield of 43.95%. Compared to ultrasonic and microwave-assisted extraction methods, infrared-assisted extraction offers several distinct advantages: (1) operational simplicity, (2) reduced reliance on complex instrumentation, and (3) minimal risk of thermal degradation. However, the method is associated with higher energy consumption during prolonged extraction processes, which may limit its industrial scalability.

**3.1.7. Deep eutectic solvents (DESSs).** Deep eutectic solvents (DESSs) represent a novel class of green solvents characterized by their unique composition of hydrogen bond donors (HBDs) and hydrogen bond acceptors (HBAs) in specific molar ratios. These solvents exhibit remarkable properties, including low melting points, negligible volatility, and excellent solvation capabilities, making them particularly suitable for the extraction of bioactive compounds.<sup>38</sup> In the extraction of *Bletilla striata* polysaccharides (BSPs), a DES system composed of choline chloride and urea in a 1 : 2 molar ratio has demonstrated superior extraction efficiency. Optimization studies revealed that the highest extraction yield (55.8%) was achieved under the following conditions: extraction time of 47 minutes,



temperature of 78 °C, DES water content of 35%, and solid–liquid ratio of 1 : 25. This represents a 36.77% improvement over conventional hot water extraction methods.<sup>39</sup> Despite their advantages, including (1) energy efficiency, (2) environmental compatibility, (3) operational simplicity, and (4) mild extraction conditions, the application of DESs in polysaccharide extraction remains relatively unexplored. Key challenges that require further investigation include (1) comprehensive safety assessments, (2) solvent recovery and reuse strategies, and (3) the impact of DES composition on polysaccharide structure and bioactivity.

### 3.2. Purification method

The crude polysaccharide extract from *Bletilla striata* typically contains various impurities, including proteins, pigments, and inorganic salts, which must be removed to obtain purified polysaccharides for structural characterization and bioactivity studies. The purification process generally involves three main steps: deproteinization, decolorization, and fractionation. Protein removal is commonly achieved through either the Sevag method or enzymatic hydrolysis. The Sevag method,<sup>48</sup> which involves the addition of a chloroform : *n*-butanol mixture (typically 4 : 1 v/v) to precipitate proteins, remains widely used due to its simplicity and effectiveness.<sup>49</sup> Enzymatic methods, while more specific, may introduce additional costs and complexity. Pigment removal is typically accomplished through activated carbon adsorption or ion-exchange chromatography. The choice of method depends on the nature and concentration of the pigments present in the crude extract. Column chromatography is the most widely employed technique for polysaccharide fractionation and purification.<sup>50</sup> Two primary chromatographic methods are commonly used: ion-exchange chromatography and gel filtration chromatography. Chen *et al.*<sup>20</sup> utilized DEAE-cellulose column chromatography with gradient elution (0.1–0.5 M NaCl) to separate BSP into three fractions (BSP-1, BSP-2, and BSP-3). Peng *et al.*<sup>25</sup> employed a combination of DEAE-cellulose-52 and Bio-Gel P-300 columns to purify BSPF-2, achieving high purity through sequential fractionation. The purification process typically concludes with concentration, dialysis, and lyophilization to obtain the final purified polysaccharide product.

## 4. Structure–activity relationship

The biological activity of plant polysaccharides is closely related to their extraction methods and structural characteristics, particularly molecular weight, monosaccharide composition, and glycosidic bond configuration.<sup>51</sup> Research has revealed significant correlations between molecular weight and bioactivity through comparative studies of various BSPs.

Wang's study demonstrated that BSP-1 with higher molecular weight exhibited superior immune activity compared to other fractions,<sup>40</sup> while Xu's research identified that high molecular weight pBSP possessed remarkable anti-fibrosis capabilities.<sup>52</sup> Conversely, studies on low molecular weight fractions showed same advantages in some biological

functions. In a comparative study, BSP-3 with the smallest molecular weight in a comparative study demonstrated the strongest antioxidant capacity, potentially attributed to its reduced molecular weight combined with elevated galactose and rhamnose content.<sup>20</sup>

Structural characteristics beyond molecular weight also significantly influence bioactivity. Chen's comparative analysis of four BSP types revealed that BSP-A's superior antioxidant capacity stemmed from its unique rough lamellar structure and  $\alpha$ -glucopyranose configuration, despite not being the lowest molecular weight fraction. This study also highlighted the complex relationship between structural integrity and bioactivity, as BSP-U's molecular weight reduction through ultrasonic treatment paradoxically diminished its reducing capacity due to glycosidic bond disruption. Further supporting this structure–function relationship,<sup>5</sup> comparative studies between pBSP and pFSP demonstrated that the latter's enhanced antioxidant activity could be attributed to its lower molecular weight and more open branched-chain architecture. These findings collectively emphasize that polysaccharide bioactivity results from the intricate interplay of multiple structural parameters.

## 5. Biological activity of *Bletilla striata* polysaccharide

### 5.1 Anti-inflammatory activity

Inflammation represents a fundamental immune defense mechanism triggered by various external stimuli, characterized by the release of pro-inflammatory cytokines and ROS. *In vivo* studies have revealed BSP's capacity to modulate cytokine production: He<sup>14</sup> found that BSP could significantly reduce the expression levels of pro-inflammatory factors TNF- $\alpha$ , IL-6 and IL-1 $\beta$  in serum. Guo<sup>53</sup> found that the level of inflammatory factors in rat gingivitis model treated with BSP was significantly regulated. Molecular mechanisms underlying these effects include: (1) ROS suppression: Yue *et al.*<sup>54</sup> demonstrated BSPb's inhibition of Ang II-induced ROS generation. (2) Cytokine regulation: downregulation of pro-inflammatory mediators (IL-6, TNF- $\alpha$ )<sup>54,55</sup> and upregulation of tight junction proteins (ZO-1, occludin) for mucosal protection.<sup>56</sup> In addition, Wang's research found that *Bletilla striata* polysaccharide can induce the proliferation and immune enhancement of vascular endothelial cells and growth factors, act on macrophages and stimulate the expression of pro-inflammatory cytokines.<sup>57</sup> These findings collectively suggest that BSPs exert anti-inflammatory effects through a complex network of immunomodulatory actions, making them promising candidates for inflammatory disorder management.

### 5.2 Hemostatic activity

Hemostasis is a vital physiological process that prevents excessive blood loss through coordinated mechanisms including vasoconstriction, platelet activation, coagulation cascade initiation, and fibrin clot formation. Growing evidence suggests that BSPs exhibit significant hemostatic properties, although their precise molecular mechanisms require further



elucidation. Current research has demonstrated that BSPs promote hemostasis through multiple pathways. Hung *et al.*<sup>58</sup> identified water-soluble BSP as a key mediator in accelerating hemostatic responses, highlighting its potential clinical utility. Further mechanistic studies by Dong *et al.*<sup>59</sup> revealed that BSP at concentrations of 50–200 mg L<sup>-1</sup> significantly enhances platelet aggregation in rat PRP in a concentration-dependent manner. This effect appears to be mediated through activation of the ADP receptor signaling pathway, specifically involving P2Y1 and P2Y12 receptors, as well as PKC, leading to platelet shape change, granule secretion, and subsequent aggregation. Additional evidence from Guo *et al.*<sup>53</sup> supports these findings, showing that BSPs effectively promote platelet aggregation and accelerate clot formation in rat gingivitis models. These observations suggest that BSPs may function through both physical adhesion properties and biochemical modulation of coagulation pathways. The mucoadhesive nature of BSPs likely facilitates platelet adhesion at injury sites, while potential interactions with fibrinogen or von Willebrand factor may contribute to clot stabilization. The promising hemostatic properties of BSPs position them as attractive candidates for various clinical applications, including surgical hemostatic agents, emergency trauma care products, and adjuncts for bleeding disorders. However, several key questions remain unanswered regarding their exact molecular targets, potential synergies with existing hemostatic agents, and the influence of structural modifications on activity.

### 5.3. Wound healing

Wound healing is a series of complex processes for the body to repair and regenerate injured tissues, involving hemostasis, inflammation, cell regeneration, tissue remodeling and other processes. Guo *et al.*<sup>53</sup> found that the sulfate of BSPs can induce PLA2, promote the release of AA in the blood to increase TXB2, thereby promoting platelet aggregation. In the study of insulin wound healing, Zhao *et al.*<sup>60</sup> found that BSP can inhibit macrophage infiltration and NLRP3 inflammasome activation, reduce IL-1 $\beta$  expression level and promote angiogenesis. These results show that BSP has the ability to promote wound healing. Zhang *et al.*<sup>61</sup> found that BSP hydrogel can promote re-epithelialization and collagen deposition, and accelerate wound healing by activating TGF- $\beta$ /Smad signaling pathway. The experimental results of He showed that the wound healing rate of the BSP treatment group was close to 85% on the 9th day after injury, which was nearly 20% higher than that of the control group, which also indicated that BSP had the ability to promote wound healing.<sup>14</sup> Wu *et al.*<sup>62</sup>'s study found that BSP can down-regulate the expression of SCEL gene, significantly reduce LPS-induced HMEC-1 cell injury and promote wound healing by promoting cell survival, reducing apoptosis, enhancing migration and angiogenesis.

### 5.4. Antioxidant activity

Oxidative stress, resulting from an imbalance between ROS production and antioxidant defenses, plays a critical role in various pathological processes. The antioxidant properties of

BSPs have been extensively investigated, demonstrating their potential as natural antioxidants. Chen *et al.*<sup>5</sup> conducted a comprehensive comparative study evaluating the antioxidant capacity of BSPs extracted through four distinct methods. Their findings revealed significant variations in free radical scavenging capabilities against DPPH, ABTS, and hydroxyl radicals among the different BSP preparations. These differences were attributed to extraction method-dependent modifications in polysaccharide structure and composition, suggesting that the extraction process significantly influences the antioxidant potential of BSPs. Further evidence from He *et al.*<sup>14</sup> demonstrated the *in vivo* antioxidant effects of BSP in murine models. Treatment with BSP resulted in a marked increase in SOD activity in both serum and liver tissues, accompanied by significant reductions in NO and MDA levels. These results demonstrate that the mechanisms by which BSP regulates oxidative stress include: (1) direct scavenging of free radicals; (2) enhancing the activity of endogenous antioxidant enzyme systems; (3) inhibiting lipid peroxidation; (4) regulating endogenous NO metabolism. The observed modulation of oxidative stress markers suggests that BSPs may offer therapeutic potential in diseases associated with oxidative damage.

### 5.5. Antimicrobial activity

Currently, research on the antibacterial activity of *Bletilla striata* polysaccharides is relatively limited. However, existing studies have demonstrated that these polysaccharides possess antibacterial activity against both Gram-positive and Gram-negative pathogens. Li *et al.*<sup>63</sup> reported concentration-dependent bactericidal activity against *Staphylococcus aureus* (6.25–12.50 mg mL<sup>-1</sup>), with mechanistic studies suggesting membrane permeability alteration as a potential mode of action. These findings were extended by Dai *et al.*,<sup>64</sup> who demonstrated inhibitory effects against *Escherichia coli*, *Proteus* spp., *Staphylococcus aureus*, and *Bacillus subtilis*, with enhanced efficacy observed at 20 mg mL<sup>-1</sup>. The consistent observation of membrane permeability changes across studies suggests this may represent a fundamental antibacterial mechanism of BSPs.

### 5.6. Other activities

Beyond its established biological activities, BSPs exhibit a broad spectrum of pharmacological effects, including immunomodulatory activity, anti-tumor activity<sup>65–67</sup> and anti-fibrosis effect,<sup>27,68</sup> as demonstrated by various *in vitro* and *in vivo* studies.

Immunomodulatory studies have revealed significant effects of BSPs on immune cell function. Peng *et al.* observed that BSP treatment could modulate the lifespan of *Pseudomonas aeruginosa*-infected nematodes and exert thymus-dependent immunoregulatory effects in mice, with BSPF2 demonstrating particularly potent activity in stimulating murine spleen cell proliferation.<sup>25</sup> Complementary findings by Liu *et al.* showed that BSAP administration in tumor-bearing rats provided protective effects on thymus and spleen organs while enhancing macrophage activity, lymphocyte proliferation, and NK cell function, along with favorable modulation of lymphocyte subpopulations.<sup>21</sup>



## 6. BSP-based composite biomaterials: benefiting from BSP bioactivity

While bioactive components with pharmacological effects offer therapeutic potential, their clinical application is often limited when used in isolation. To address these limitations and meet clinical requirements, the development of composite biomaterials has emerged as a promising strategy. In biomedical research, composite biomaterials have gained significant attention due to their ability to integrate the advantages of multiple components through physical or chemical cross-linking, thereby overcoming the constraints of individual materials while enhancing overall functionality. The growing recognition of BSPs diverse biological activities has spurred increasing interest in their incorporation into composite biomaterials for advanced biomedical applications. Recent studies have focused on developing BSP-based composite systems that leverage its inherent bioactivity while combining it with other functional materials to achieve synergistic effects. Currently, several composite biomaterials containing BSP have been studied, including gel-based biomaterials for wound healing and drug delivery, hemostatic cotton formulations for rapid blood coagulation, microneedle systems for transdermal applications, composite eye drops for ophthalmic treatment, and film materials with good mechanical properties. These composite materials capitalize on BSP's unique properties while addressing specific clinical needs. Table 3 provides a comprehensive overview of current BSP-based composite biomaterials, including their compositions, fabrication methods, and intended applications. The development of such composite systems represents an important step toward translating BSP's pharmacological potential into clinically viable products, with ongoing research focusing on optimizing material properties, enhancing bioactivity, and ensuring safety for human use. Future directions include the exploration of novel composite formulations and the refinement of fabrication techniques to further expand BSP's biomedical applications.

### 6.1. Physicochemical property

As a typical plant-derived polysaccharide, BSP exhibits excellent biocompatibility and biodegradability; it can be enzymatically degraded into monosaccharides and completely metabolized *in vivo*, eliminating the risk of by-product accumulation and providing a prerequisite for its use as an implantable biomaterial. CCK-8 cytotoxicity assays showed no significant cytotoxic or inhibitory effects on IEC-18 cells at concentrations of 25, 50 and 100  $\mu\text{g mL}^{-1}$ , demonstrating good biosafety.<sup>56</sup> Moreover, comparative studies reveal that BSP-based biomaterials offer a markedly superior safety profile to conventional materials.<sup>69</sup>

BSP is composed mainly of mannose and glucose, and its side chains are rich in hydroxyl groups with a small number of carboxyl and amino substituents. This structure endows the polysaccharide with excellent hydrophilicity and multiple cross-linking options: periodate oxidation rapidly generates aldehyde

groups that undergo Schiff-base gelation with amino-bearing polymers within seconds, while methacrylation enables photo-cross-linking under specific light doses. The viscosity of BSP solutions increases with molecular weight, and film strength rises accordingly, allowing mechanical properties to be tuned for a variety of applications.<sup>70</sup> In addition to its favorable rheological profile, BSP exhibits inherent mucoadhesivity, offering the potential for prolonged residence and targeted interaction with mucosal tissues. The 3D helical conformation of BSP exposes numerous hydroxyl and ether-oxygen groups, enabling multipoint hydrogen bonding with mucins for robust mucosal adhesion, while the central helical cavity can simultaneously encapsulate hydrophobic drugs, integrating firm attachment and drug-loading functions in a single platform.<sup>71</sup> Pharmacologically, as outlined earlier, extensive studies have demonstrated that BSP possesses potent anti-inflammatory, repair-promoting and antimicrobial activities. Whether used alone as the principal therapeutic ingredient or as a functional excipient, it offers significant value; detailed bioactivity applications will be elaborated in the following sections according to biomaterial categories.

In short, both its physicochemical behavior and chemical structure underscore BSP as a highly promising raw material for biomaterial synthesis.

### 6.2. Cross-link

The dense array of hydroxyl groups and oxidizable vicinal diols on the BSP backbone provides the key reactive handles for cross-linking: oxidation furnishes aldehydes for Schiff-base covalent assembly, hydroxyls can be esterified to form covalent ester bonds, and the same diol/carboxylic motifs coordinate multivalent metal ions. Both physical and chemical cross-linking pathways are therefore accessible during BSP biomaterial fabrication; the detailed mechanisms are elaborated in the following two sections.

**6.2.1. Chemical cross-link.** Chemical crosslinking is a key strategy for integrating two or more individual polymers into a composite, imparting enhanced stability and mechanical strength through covalent bonding while preserving biocompatibility.<sup>71</sup> The Schiff-base reaction is a widely employed chemical cross-linking strategy in which primary amines condense with aldehyde or ketone groups at neutral pH to form reversible imine bonds. Dehydration-driven and dynamically cleavable within the tissue micro-environment, these imine linkages endow hydrogels and scaffolds with both degradability and cytocompatibility.<sup>72,73</sup> Photocrosslinking is another prevalent chemical cross-linking modality: a photoinitiator activated by a specific wavelength generates reactive radicals that rapidly form covalent bonds with polymer chains, yielding no by-products and completing within seconds.<sup>74,75</sup> Oxalyl chloride-mediated covalent cross-linking has also been exploited by several groups, the reaction proceeds without residual aldehydes and exhibits minimal cytotoxicity, making it an advantageous cross-linking tool for hemostatic sponges.<sup>76</sup>

**6.2.2. Physical cross-link.** In contrast to chemical cross-linking, physical cross-linking assembles three-dimensional





Table 3 Composite biomaterials based on the biological activity of BSP

Name	Biomaterial compositions	Crosslinking	Property	Application potential	Ref.
<b>Gels</b>					
Methacrylate-modified chitosan and ferulic acid and OBSP combined multi-functional spray hydrogel	Methacrylate-modified chitosan; ferulic acid; OBSP	Chemical photocrosslinking	Antibacterial activity; biocompatibility; antioxidant activity; hemostatic activity	Spray-based hydrogel for promoting wound healing	81
<i>Bletilla striata</i> polysaccharide/chitosan hydrogel	BSP; chitosan	Chemical crosslinking of schiff base reaction	Biodegradability; biocompatibility	Hydrogel nanoparticles	83
A dual network cross-linked hydrogel with multifunctional <i>Bletilla striata</i> polysaccharide/gelatin/tea polyphenol	OBSP; tea polyphenol; adipic acid dihydrazide modified gelatin	Chemical crosslinking of schiff base reaction	Antioxidant; antimicrobial; hemostatic properties	Double network crosslinked hydrogel for promoting wound healing	95
Ligand-selective targeting of macrophage hydrogel	BSP; gelatin; mesoporous bioactive glass	Chemical crosslinking of schiff base reaction	Biocompatibility; promoting intraosseous; self-repair	Macrophage hydrogel	84
A blend hydrogel of polysaccharide	BSP; curdlan-based hydrogel	Physical crosslinking of heating-cooling	Biocompatibility; wound healing	Curdlan-based hydrogel for wound healing	85
A multifunctional herb-derived glycopeptide hydrogel	OBSP; gallic acid-grafted -polylysine; dpaoniflorin-loaded micelles	Chemical crosslinking of schiff base reaction	Injectability; self-healing; biocompatibility	Multifunctional herb-derived glycopeptide hydrogel	96
Multi-functional dual network polysaccharide hydrogel	OBSP; gallic acid grafted chitosan	Schiff base and pyrogallol-Fe <sup>3+</sup>	Self-healing; biocompatibility;	Dual network polysaccharide hydrogel adhesive	80
Physical dual-network photothermal antibacterial multifunctional hydrogel	BSP-U; dopamine-conjugated di-aldehyde-hyaluronic linked with Fe <sup>3+</sup>	Chemical cross-linking of Fe <sup>3+</sup> under alkaline conditions	Anti-oxidant; biocompatibility;	Multifunctional hydrogel adhesive	97
Deformable sodium alginate/ <i>Bletilla striata</i> polysaccharide <i>in situ</i> gel	Sodium alginate; deacetylated gellan gum; calcium citrate; BSP	Physical crosslinking of heating and cooling	Deformability; mechanical resistance; bioadhesion; gastric retention	Gastric acid-sensitive <i>in situ</i> gel	78
A self-healing hydrogel wound dressing based on oxidized <i>Bletilla striata</i> polysaccharide and cationic gelatin	OBSP; cationic gelatin	Chemical crosslinking of schiff base reaction	Hemostatic activity; antioxidant activity	Hydrogel wound dressing	98
A rapid-floating natural polysaccharide gel-raft	BSP; glyceryl monooleate	Physical crosslinking by swelling method	Anti-inflammatory activity; suspension;	Polysaccharide raft for the treatment of gastroesophageal reflux disease	71
Mussel-inspired pH-responsive hydrogel based on <i>Bletilla striata</i> polysaccharide	Carboxymethylated BSP-dopamine conjugate	Chemical crosslinking of NaIO <sub>4</sub> oxidation	Cytocompatibility; hemocompatibility; antioxidant activity; antibacterial properties	As a PH-responsive drug release agent	99
<b>Sponges</b>					
<i>Bletilla striata</i> polysaccharide and chitosan composite hemostatic sponge (BSP-CS)	BSP; chitosan	Chemical cross-linking of oxalyl chloride	Antibacterial activity; hemostatic activity	Hemostatic sponge	76
<i>Bletilla striata</i> polysaccharide collagen sponge	EBSP; collagen	Chemical crosslinking catalyzed by alkaline	Blood compatibility; cytocompatibility	As a new hemostatic sponge material	86



Table 3 (Contd.)

Name	Biomaterial compositions	Crosslinking	Property	Application potential	Ref.
<b>Microneedles</b>					
Multifunctional natural microneedles based methacrylated <i>Bletilla striata</i> polysaccharide	Peony leaf extract; fmethacrylated <i>Bletilla striata</i> polysaccharide;	Chemical photocrosslinking	Antimicrobial activity; mechanical properties; biocompatibility;	For the treatment of infectious wound dressings	75
Bilayer microneedles based on <i>Bletilla striata</i> polysaccharide containing asiaticoside	Asiaticoside; BSP/(CS) com- posite bilayer dissolvable microneedles	—	Antibacterial; biocompatibility; biodegradability	Improve skin regeneration and inhibit scar formation	87
Chitosan/BSP composited microneedles	Chitosan; tannic acid; AgNO <sub>3</sub> ; BSP	—	Anti-inflammatory activity; antioxidant activity; anti-biofilm properties	Composited microneedles for infected and susceptible wound healing	100
<i>Bletilla striata</i> polysaccharide microneedles	Hyaluronic acid; polyvinyl alcohol; BSP	—	Stability; biocompatibility; safety	<i>Bletilla striata</i> polysaccharide microneedle for transdermal delivery of the vaccine	101
Novel <i>Bletilla striata</i> polysaccharide microneedles	—	—	Stability; moldability; safety	As a new transdermal drug delivery route	102
A microneedlemediated biomimetic transdermal drug delivery system	—	—	Physical stability; mechanical strength	An active targeted drug delivery system for the local treatment of hypertrophic scar fibroblasts	103
<b>Eye drops</b>					
Oxidized <i>Bletilla striata</i> polysaccharide-natamycin eye drops	BSP; NAP	Chemical crosslinking of schiff base reaction	Biocompatibility; anti-inflammatory activity; safety	As a compound eye drops for the treatment of deep eye ulcers	73
Levofloxacin-BSP eye drops	BSP; levofloxacin	—	Antibacterial; biocompatibility;	As a local eye drug delivery carrier	91
<b>Films</b>					
BSP/WPU nanofiber membrane	BSP; waterborne polyurethane	—	Anti-inflammatory activity; biocompatibility	Nerve wrapping membrane for peripheral nerve repair	92
BSP/PLA film	BSP; polylactic acid	Physical blending with 1,4-dioxane and ultrapure water as solvent	Mechanical strength; stability	New heat-resistant, low-cost and environmentally friendly composite film	93
pH/enzyme dual sensitive Gegenqinlian pellets coated with <i>Bletilla striata</i> polysaccharide membranes	BSP	—	Anti-inflammatory activity; mechanical strength; stability	Protective film for drug delivery	94

polymer networks through non-covalent interactions—hydrogen bonding, electrostatic attraction, ionic coordination and so forth. Operating under mild conditions, it leaves no chemical residues and offers reversible, stimuli-responsive behavior. These features make it the method of choice for biologically demanding applications such as biodegradable hemostats, injectable hydrogels, and gastric floating rafts.<sup>77</sup> Physical cross-linking *via* heating-cooling disrupts pre-existing hydrogen bonds at elevated temperature and rebuilds them during subsequent cooling, enabling a reversible “sol-on-

heating, gel-on-cooling” transition.<sup>78</sup> Physical cross-linking *via* the swelling approach allows pre-existing junctions within a dry network to rearrange and densify upon hydration, forming additional hydrogen bonds that convert a dry wafer into a hydrogel in a single step.<sup>71</sup> Metal-ion coordination cross-linking—although it creates chemical coordinate bonds—operates with bond energies far below those of covalent linkages and is therefore classified as a physical cross-linking strategy.<sup>79,80</sup>



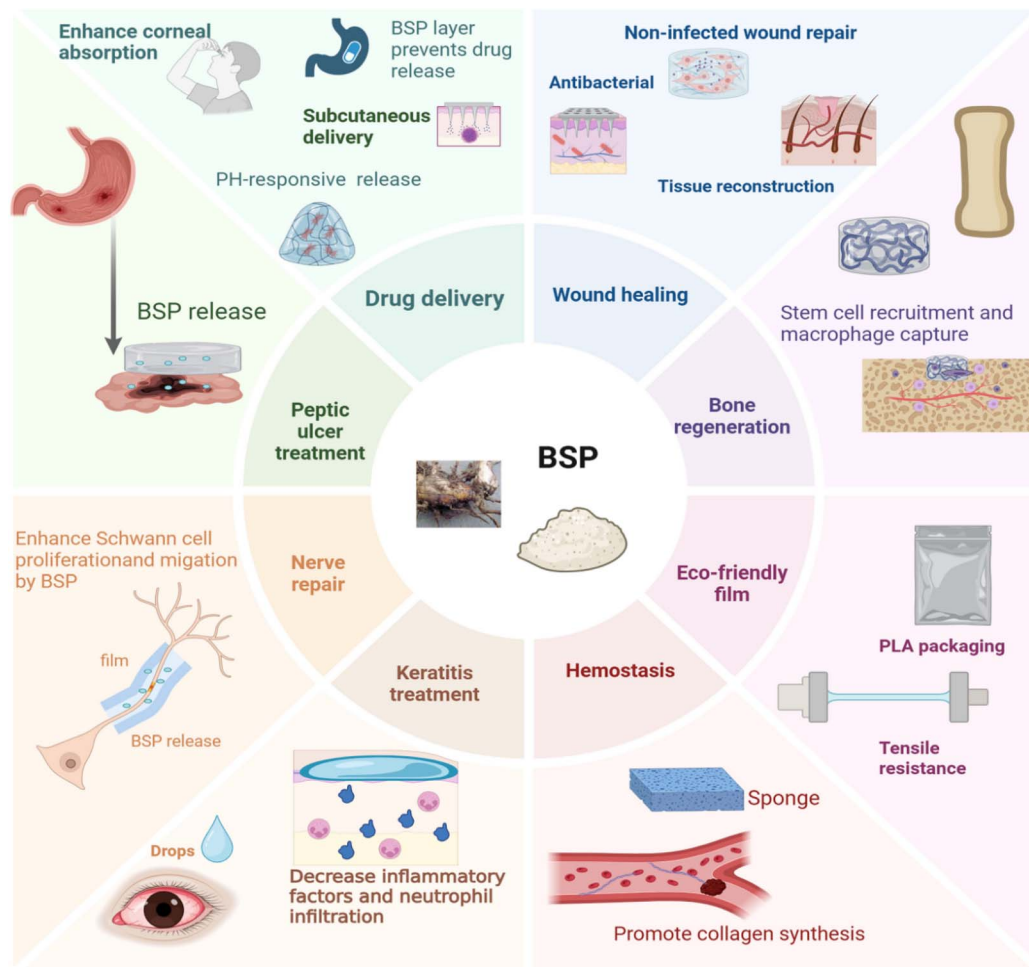


Fig. 3 Application potential and mechanism of action of bio-materials based on the bioactivity of BSPs.

### 6.3. Biomaterials

**6.3.1. Gels.** Hydrogels have emerged as particularly promising platforms for clinical wound healing applications due to their tunable physical properties and ability to mimic the extracellular matrix. These three-dimensional networks can be fabricated through various crosslinking strategies, including thermal-induced gelation, photo-crosslinking, and chemical conjugation. Among these, chemical crosslinking *via* Schiff base formation between amine groups and oxidized polysaccharides has become a predominant approach for creating BSP-based hydrogels, owing to its mild reaction conditions and reversible imine bonding.

Recent advances in BSP hydrogel design have yielded sophisticated systems with multifunctional capabilities. Zhong *et al.*<sup>81</sup> developed an innovative sprayable hydrogel system through the Schiff base reaction between OBSP and methacrylate-modified chitosan/ferulic acid complexes. This dynamic hydrogel demonstrated exceptional performance in irregular wound management, combining antibacterial, antioxidant, and hemostatic properties with controlled degradability. Yang<sup>82</sup>'s subsequent modification incorporating plant-derived bacilli further enhanced the antimicrobial efficacy of

this platform, showcasing the versatility of this design approach.

For gastrointestinal applications, researchers have engineered temperature-sensitive adhesive hydrogels by cross-linking oxidized BSP with chitosan and  $\beta$ -glycerophosphate. This intelligent system undergoes rapid sol-gel transition at physiological temperatures, forming a nanoparticle-loaded hydrogel that adheres effectively to ulcerative colitis lesions while prolonging drug release through enhanced mucosal retention. The system's prolonged residence time in the harsh gastrointestinal environment represents a significant advancement in local drug delivery for inflammatory bowel disease.<sup>83</sup>

In bone tissue engineering, Wang *et al.*<sup>84</sup> created a novel GBMgel through Schiff base-mediated self-assembly. This composite material demonstrates unique immunomodulatory properties, capable of macrophage recruitment and polarization through modulation of TLR4/NF- $\kappa$ B, MAPK, and JAK/STAT3 signaling pathways. The resulting pro-regenerative immune microenvironment promotes osteogenic differentiation and bone defect repair, highlighting BSP's potential in immunoinstructive biomaterials.

Simpler yet effective systems have also been developed, such as Shang<sup>85</sup>'s thermally crosslinked BSP-curdlan blend hydrogel.



This straightforward preparation yields materials with excellent biocompatibility and wound healing performance, demonstrating that even minimally processed BSP composites can achieve significant therapeutic effects. The versatility of BSP-based hydrogels is further evidenced by their capacity for functional augmentation through incorporation of antimicrobial agents, growth factors, or other therapeutic compounds. This modular design approach enables precise tailoring of material properties to meet specific clinical requirements, paving the way for personalized wound care solutions. Current research continues to explore novel combinations of BSP with both natural and synthetic polymers to optimize mechanical properties, degradation kinetics, and bioactive compound release profiles for enhanced therapeutic outcomes.

**6.3.2. Sponges.** Effective hemostasis represents the critical first phase of successful wound healing, and advanced hemostatic materials must combine rapid clotting capability with biocompatibility to minimize complications. Hemostatic sponges have emerged as particularly valuable in this regard, offering the dual advantages of traditional coagulation promotion coupled with superior fluid absorption capacity for blood and wound exudates.

Recent innovations in BSP-based sponge composites have significantly advanced hemostatic material performance. Zhang *et al.*<sup>76</sup> developed a novel chitosan-BSP composite sponge through oxalyl chloride-mediated crosslinking, which demonstrated marked improvements over conventional gauze across multiple hemostatic parameters. Experimental evaluations revealed superior performance in: hemostasis time, *in vitro* coagulation time, blood loss volume and antimicrobial activity. Parallel work by Tang *et al.*<sup>86</sup> employed an alternative chemical strategy, creating EBSP for crosslinking with collagen under alkaline conditions. The resulting EBSP-collagen sponge exhibited exceptional blood and cell compatibility while maintaining robust hemostatic performance. Comparative studies with standard gauze demonstrated: enhanced platelet adhesion and activation, improved fibrin network formation, reduced inflammatory response and sustained structural integrity in wet conditions.

Although hemostatic sponges have been commonly used hemostatic materials, it is still meaningful to study new composite sponges on the basis of traditional hemostatic sponge materials, which can solve the problems of limited hemostatic efficiency, poor biocompatibility and infection risk of traditional sponges.

**6.3.3. Microneedles.** Microneedle arrays represent an innovative transdermal drug delivery platform that overcomes the skin's formidable barrier properties while avoiding the pain associated with conventional hypodermic injections. These microscale devices create temporary conduits through the stratum corneum, enabling efficient drug transport to subcutaneous tissues while minimizing tissue damage. Recent developments have incorporated BSP into microneedle systems, capitalizing on its unique physicochemical and biological properties to enhance therapeutic outcomes.

Lv *et al.*<sup>87</sup> engineered a sophisticated bilayer soluble microneedle system composed of BSP and CS for AS delivery. This

design addressed AS's pharmacological limitations – poor water solubility and suboptimal lipophilicity – by utilizing BSP as both a drug carrier and functional excipient. The CS-AS-BSP microneedles demonstrated controlled drug release kinetics while providing complementary anti-inflammatory and tissue repair benefits from BSP. Comprehensive *in vitro* and *in vivo* evaluations confirmed the system's excellent antibacterial properties, biocompatibility, and biodegradability, establishing a promising platform for scar prevention and wound management. Further advancing this technology, Ye *et al.*<sup>75</sup> developed a photocrosslinkable microneedle system using BSPMA and CSMA incorporated with PLE. The resulting BCP-MN composite exhibited exceptional mechanical properties for reliable skin penetration while maintaining structural integrity during drug delivery. This multifunctional system addressed key challenges in treating deep skin infections through its demonstrated capabilities in bacterial inhibition and reactive oxygen species scavenging. The incorporation of BSPMA provided enhanced structural stability and bioactive functionality compared to conventional microneedle formulations.

As a new type of composite material, microneedle has less research on its clinical application than other biomaterials. Its unique physical structure can achieve subcutaneous high-efficiency treatment and has good application prospects.

**6.3.4. Eye drops.** The BSP in ophthalmic drug delivery has emerged as a promising strategy to overcome the challenges of conventional ocular treatments. Despite the extensive study of polysaccharides for ocular applications,<sup>88,89</sup> however, there are few studies based on BSP. Recent studies have demonstrated the potential of BSP to improve the efficacy of ocular drugs, particularly in treating deep corneal infections that are difficult to manage with traditional formulations.

A significant advancement was achieved by Tian *et al.*,<sup>73</sup> who developed OBN through Schiff base crosslinking. This innovative formulation addressed the major limitations of natamycin, a potent antifungal agent whose clinical use has been restricted by poor water solubility and inadequate penetration into the corneal stroma. The OBN system not only enhanced drug solubility but also facilitated deeper tissue penetration, significantly improving therapeutic outcomes in fungal keratitis. Similarly, Wu *et al.*<sup>90,91</sup> demonstrated that combining BSP with levofloxacin resulted in superior antibacterial efficacy against *Staphylococcus aureus*-induced keratitis compared to levofloxacin alone. The BSP component was shown to promote drug penetration into the corneal stroma while contributing additional pharmacological benefits.

The effectiveness of BSP in ocular drug delivery stems from its unique physicochemical properties. Its mucoadhesive nature prolongs residence time on the ocular surface, while its structural characteristics enhance drug permeation across corneal barriers. Furthermore, safety studies involving subconjunctival injection of BSP have confirmed its excellent tissue compatibility, supporting its potential as a safe and effective carrier for ocular therapeutics. These findings highlight the versatility of BSP-based formulations, which could be adapted for various ocular conditions, including bacterial and fungal infections, as well as inflammatory disorders.





**6.3.5. Film.** Composite films incorporating BSP have demonstrated remarkable potential in biomedical applications due to their enhanced stability and tunable mechanical properties. Recent developments in BSP-based film technologies have yielded materials with multifunctional capabilities, ranging from neural regeneration to gastrointestinal therapeutics.

Chen *et al.*<sup>92</sup> engineered a novel nanofiber membrane (NFM) by combining BSP with water-based polyurethane (WPU), creating a composite material that synergistically combines structural support with biological activity. This innovative membrane demonstrated significant benefits in peripheral nerve repair, where it promoted Schwann cell proliferation and axon regeneration while preventing tissue adhesion. The dual functionality of the BSP-WPU composite – providing both mechanical guidance and anti-inflammatory support – represents a substantial advancement in neural tissue engineering materials. Yang *et al.*<sup>93</sup> developed a BSP-poly(lactic acid) (PLA) composite film through solvent blending techniques. This formulation exhibited notable improvements in thermal stability and mechanical performance, with a significant elevation in glass transition temperature compared to pure PLA. The enhanced tensile strength and thermal properties of this biocomposite suggest promising applications in medical devices and packaging where both durability and biodegradability are required. Sun<sup>94</sup>'s work on pH/enzyme dual-responsive drug delivery systems showcased another innovative application of BSP films. By coating Gegen Qinlian pellets with BSP, researchers created an intelligent delivery vehicle for treating gastrointestinal ulcers. The BSP coating not only provided robust mechanical protection but also contributed anti-inflammatory activity to the therapeutic payload. This system's ability to respond to both pH changes and enzymatic activity in the gastrointestinal tract demonstrates the versatility of BSP-based films in controlled drug delivery applications. The development of these advanced film materials highlights BSP's unique capacity to enhance both the physical properties and biological functionality of biomedical composites.

Regarding the clinical application potential of composite materials synthesized from different materials, Fig. 3 provides visual presentation and support.

## 7. Conclusion and prospect

As a medicinal plant that has been used in traditional Chinese medicine for thousands of years, *Bletilla striata* has garnered increasing scientific interest due to its rich bioactive components, particularly BSPs. These polysaccharides exhibit a complex structural configuration, including the characteristic triple-helix conformation, though their complete structural elucidation remains an active area of research. The extraction of BSP has evolved from conventional methods such as hot water and alkaline extraction to more advanced techniques, including ultrasound-, microwave-, infrared-, and enzyme-assisted approaches. While these modern methods offer improved efficiency and reduced environmental impact, they also present challenges such as equipment costs and process optimization.

The integration of multiple techniques in hybrid extraction shows potential for increasing yield while maintaining biological activity, thus paving the way for more sustainable and scalable production methods. The integration of multiple techniques in hybrid extraction shows potential for increasing yield while maintaining biological activity, thus paving the way for more sustainable and scalable production methods.

The pharmacological potential of BSP is vast, with demonstrated efficacy in anti-inflammatory, wound healing, hemostatic, and antioxidant applications. Recognizing the limitations of BSP in isolation, researchers have increasingly turned to composite biomaterials—such as hydrogels, sponges, microneedles, eye drops and films—that integrate BSP with other functional components to enhance bioactivity and mechanical properties. These advanced materials exhibit excellent biocompatibility, anti-infection capabilities, and tissue repair promotion, offering significant improvements over traditional wound treatments. Moreover, they hold promise for personalized medicine by enabling tailored therapeutic solutions.

Despite these advancements, the path to clinical adoption necessitates rigorous evaluation of safety, environmental impact, and long-term efficacy. Future research should focus on standardizing extraction and fabrication protocols, optimizing material performance for specific medical applications, and conducting comprehensive preclinical and clinical validations. Additionally, exploring novel applications in drug delivery, regenerative medicine, and immune modulation could further expand the utility of BSP-based biomaterials. By addressing these challenges, BSP-derived composites have the potential to revolutionize wound care and other biomedical fields, bridging traditional medicine with modern therapeutic innovation.

## Author contributions

J. F.: writing—original draft preparation; Y. L.: writing—review; N. X., K. H.: investigation; T. C.: editor; S. C., R. F.: supervision and conceptualization. All authors have read and agreed to the published version of the manuscript.

## Conflicts of interest

There are no conflicts to declare.

## Abbreviations

AS	Asiaticoside
ABTS	3-Ethylbenzothiazoline-6-sulphonic acid
BSPMA	Methacrylated <i>Bletilla striata</i> polysaccharide
BBD	Box–Behnken design
CSMA	Methacrylated chitosan
CS	Chitosan
DESS	Deep eutectic solvents
DPPH	1,1-Diphenyl-2-picrylhydrazyl
EBSP	Epoxy <i>Bletilla striata</i> polysaccharide
GPC	Gel permeation chromatography



Glc	Glucose
Gal	Galactose
GC	Gas chromatography
GA-BP	Genetic algorithm-back-propagation
GBMgel	Gelatin- <i>Bletilla striata</i> polysaccharide-mesoporous bioactive glass hydrogel
GC-MS	Gas chromatography-mass spectrometry
HBDs	Hydrogen bond donors
HBAs	Hydrogen bond acceptors
HMEC-1	Human microvascular endothelial cells
HPGPC	High-performance gel permeation chromatography
IC	Ion chromatography
JAK/STAT3	Janus kinase/signal transducer and activator of transcription 3
LPS	Lipopolysaccharide
$M_n$	Number-average molecular weight
$M_w$	Weight-average molecular weight
MALLS	Multi-angle laser light scattering
Man	Mannose
MAPK	Mitogen-activated protein kinase
MDA	Malondialdehyde
NK	Natural killer
NMR	Nuclear magnetic resonance
NFM	Nanofiber membrane
NO	Nitric oxide
OBSP	Oxidized BSP
OBN	Oxidized <i>Bletilla striata</i> polysaccharide-natamycin conjugates
PRP	Platelet-rich plasma
PKC	Protein kinase C
PLE	Peony leaf extract
PLA	Poly(lactic acid)
RI	Refractive index
RSM	Response surface methodology
ROS	Reactive oxygen species
SEC	Size exclusion chromatography
SCEL	Synaptopodin-2-like gene
SOD	Superoxide dismutase
WPU	Water-based polyurethane
Xyl	Xylose

## Data availability

No primary research results, software or code have been included and no new data were generated or analysed as part of this review.

## Acknowledgements

This research was funded by the National Natural Science Foundation of China (No. 82304714, 330020057), PhD Start-up Foundation of Liaoning Province (2024-BS-274), Basic Research Projects of Liaoning Provincial Department of Education (No. JYTMS20231406), Liaoning Province Science and Technology Innovation Team Project (No. LJ222410164015) and National College Student Innovation Training Project, China (No. 20239007).

## References

- 1 K. W. Tan, *Brittonia*, 1969, **21**, 202–214.
- 2 E. C. O. F. R. P. Sinicae, *Flora Reipublicae Popularis Sinicae*, Science Press, Beijing, 1999.
- 3 S. Jiang, M. Wang, L. Jiang, Q. Xie, H. Yuan, Y. Yang, S. Zafar, Y. Liu, Y. Jian, B. Li and W. Wang, *J. Ethnopharmacol.*, 2021, **280**, 114263.
- 4 W. Zhai, E. Wei, R. Li, T. Ji, Y. Jiang, X. Wang, Y. Liu, Z. Ding and H. Zhou, *ACS Omega*, 2021, **6**, 656–665.
- 5 H. Chen, J. Zeng, B. Wang, Z. Cheng, J. Xu, W. Gao and K. Chen, *Carbohydr. Polym.*, 2021, **266**, 118149.
- 6 H. Diao, X. Li, J. Chen, Y. Luo, X. Chen, L. Dong, C. Wang, C. Zhang and J. Zhang, *J. Biosci. Bioeng.*, 2008, **105**, 85–89.
- 7 X. Yang, C. Tang, P. Zhao, G. Shu and Z. Mei, *Planta Med.*, 2012, **78**, 606–610.
- 8 W. Wang and H. Meng, *Fitoterapia*, 2015, **101**, 12–18.
- 9 Y. Shi, B. Zhang, Y. Lu, C. Qian, Y. Feng, L. Fang, Z. Ding and D. Cheng, *BMC Complementary Altern. Med.*, 2017, **17**, 273.
- 10 A. Sun, J. Liu, S. Pang, J. Lin and R. Xu, *Bioorg. Med. Chem. Lett.*, 2016, **26**, 2375–2379.
- 11 B. Wang, H. Zhang, L. Chen, Z. Mi, Y. Xu and G. Zhao, *Carbohydr. Polym.*, 2020, **246**, 116620.
- 12 G. Jiang, B. Wang, Y. Wang, H. Kong, Y. Wang, P. Gao, M. Guo, W. Li, J. Zhang, Z. Wang and J. Niu, *Carbohydr. Polym.*, 2023, **313**, 120781.
- 13 C. L. Lee, Y. L. Jhan, H. M. Chiang and C. J. Chen, *Nat. Prod. Res.*, 2024, **38**, 3848–3853.
- 14 X. He, L. Liu, F. Gu, R. Huang, L. Liu, Y. Nian, Y. Zhang and C. Song, *Int. J. Biol. Macromol.*, 2024, **261**, 129874.
- 15 I. Kwiecień and M. Kwiecień, *Gels*, 2018, **4**(2), 47.
- 16 Q. Li, Y. Niu, P. Xing and C. Wang, *Chin. Med.*, 2018, **13**, 7.
- 17 X. He, X. Wang, J. Fang, Z. Zhao, L. Huang, H. Guo and X. Zheng, *J. Ethnopharmacol.*, 2017, **195**, 20–38.
- 18 Z. Zhu, T. Liang, G. Dai, J. Zheng, J. Dong, C. Xia and B. Duan, *Int. J. Biol. Macromol.*, 2023, **245**, 125407.
- 19 J. Xu, S. L. Li, R. Q. Yue, C. H. Ko, J. M. Hu, J. Liu, H. M. Ho, T. Yi, Z. Z. Zhao, J. Zhou, P. C. Leung, H. B. Chen and Q. B. Han, *Anal. Bioanal. Chem.*, 2014, **406**, 6409–6417.
- 20 H. Chen, Y. Wu, B. Wang, M. Kui, J. Xu, H. Ma, J. Li, J. Zeng, W. Gao and K. Chen, *Int. J. Biol. Macromol.*, 2024, **262**, 130016.
- 21 C. Liu and A. J. Liu, *Chem. Biodiversity*, 2022, **19**, e202200635.
- 22 J. Qiu, X. Xu, J. Guo, Z. Wang, J. Wu, H. Ding, Y. Xu, Y. Wu, Q. Ying, J. Qiu, S. Wu and S. Shi, *Int. J. Biol. Macromol.*, 2024, **263**, 130267.
- 23 F. Huang, Y. Fan, X. Liu, Y. Chen, Y. Huang, Y. Meng and Y. Liang, *Int. J. Biol. Macromol.*, 2024, **273**, 133206.
- 24 Z. Chen, Y. Zhao, M. Zhang, X. Yang, P. Yue, D. Tang and X. Wei, *Carbohydr. Polym.*, 2020, **227**, 115362.
- 25 Q. Peng, M. Li, F. Xue and H. Liu, *Carbohydr. Polym.*, 2014, **107**, 119–123.
- 26 Y. Li, Y. Hao, X. Yang, J. Zhao, R. Chang, B. Wang and X. Zhan, *Int. J. Biol. Macromol.*, 2025, **307**, 141904.



- 27 Y. Wang, D. Liu, S. Chen, Y. Wang, H. Jiang and H. Yin, *Fitoterapia*, 2014, **92**, 72–78.
- 28 C. Wang, J. Sun, Y. Luo, W. Xue, H. Diao, L. Dong, J. Chen and J. Zhang, *Biotechnol. Lett.*, 2006, **28**, 539–543.
- 29 M. Zhao, Z. Guan, N. Tang and Y. Cheng, *Int. J. Biol. Macromol.*, 2023, **235**, 123925.
- 30 H. Chen, B. Wang, J. Li, J. Xu, J. Zeng, W. Gao and K. Chen, *Int. J. Biol. Macromol.*, 2023, **226**, 982–995.
- 31 J. Ai, Z. Yang, J. Liu, H. A. Schols, M. Battino, B. Bao, L. Tian and W. Bai, *J. Agric. Food Chem.*, 2022, **70**, 3654–3665.
- 32 X. Han, H. Liu, Y. Zhang, Y. Zhang, Z. Song, L. Yang, X. Liu, L. Yang, M. Wu and L. Tan, *Prep. Biochem. Biotechnol.*, 2024, 1–11, DOI: [10.1080/10826068.2024.2419862](https://doi.org/10.1080/10826068.2024.2419862).
- 33 J. H. Sun, J. S. Shi, D. F. Sun and W. M. Zhang, *Food Sci.*, 2009, **30**, 5.
- 34 L. Shen, S. Pang, M. Zhong, Y. Sun, A. Qayum, Y. Liu, A. Rashid, B. Xu, Q. Liang, H. Ma and X. Ren, *Ultrason. Sonochem.*, 2023, **101**, 106646.
- 35 A. Delazar, L. Nahar, S. Hamedeyazdan and S. D. Sarker, *Methods Mol. Biol.*, 2012, **864**, 89–115.
- 36 C. H. Zhang, Y. H. Yun, W. Fan, Y. Z. Liang, Y. Yu and W. X. Tang, *Int. J. Biol. Macromol.*, 2015, **79**, 983–987.
- 37 Y. Qu, C. Li, C. Zhang, R. Zeng and C. Fu, *Carbohydr. Polym.*, 2016, **148**, 345–353.
- 38 O. V. Morozova, I. S. Vasil'eva, G. P. Shumakovich, E. A. Zaitseva and A. I. Yaropolov, *Biochemistry*, 2023, **88**, s150–s175.
- 39 L. Luo, W. Fan, J. Qin, S. Guo, H. Xiao and Z. Tang, *Molecules*, 2023, **28**(14), 5538.
- 40 Y. Wang, S. Han, R. Li, B. Cui, X. Ma, X. Qi, Q. Hou, M. Lin, J. Bai and S. Li, *Int. J. Biol. Macromol.*, 2019, **122**, 628–635.
- 41 Z. Liao, R. Zeng, L. Hu, K. G. Maffucci and Y. Qu, *Int. J. Biol. Macromol.*, 2019, **122**, 1035–1045.
- 42 B. Wang, H. Zhang, L. Chen, Z. Mi, Y. Xu, G. Zhao, S. Liu, H. Lei, Z. Wang and J. Niu, *Carbohydr. Polym.*, 2020, **246**, 116620.
- 43 C. Zhang, F. Gao, S. Gan, Y. He, Z. Chen, X. Liu, C. Fu, Y. Qu and J. Zhang, *Food Chem. Toxicol.*, 2019, **131**, 110539.
- 44 M. Zhang, L. Sun, W. Zhao, X. Peng, F. Liu, Y. Wang, Y. Bi, H. Zhang and Y. Zhou, *Molecules*, 2014, **19**, 9089–9100.
- 45 C. Liu, K. Y. Dai, H. Y. Ji, X. Y. Jia and A. J. Liu, *Int. J. Biol. Macromol.*, 2022, **205**, 553–562.
- 46 L. Kong, L. Yu, T. Feng, X. Yin, T. Liu and L. Dong, *Carbohydr. Polym.*, 2015, **125**, 1–8.
- 47 Q. Yan, X. Long, P. Zhang, W. Lei, D. Sun and X. Ye, *Carbohydr. Polym.*, 2022, **293**, 119696.
- 48 Z. Y. Chen, S. H. Chen, C. H. Chen, P. Y. Chou, C. C. Yang and F. H. Lin, *Polymers*, 2020, **12**(11), 2567.
- 49 G. L. Huang, Q. Yang and Z. B. Wang, *Z. Naturforsch., C: J. Biosci.*, 2010, **65**, 387–390.
- 50 G. A. Morris, G. G. Adams and S. E. Harding, *Food Hydrocolloids*, 2014, **42**, 318–334.
- 51 A. Hussain, *Int. J. Biol. Macromol.*, 2025, **309**, 142802.
- 52 J. Xu, Z. Chen, P. Liu, Y. Wei, M. Zhang, X. Huang, L. Peng and X. Wei, *Int. J. Biol. Macromol.*, 2021, **193**, 2281–2289.
- 53 Q. Guo, B. Li, C. Bao, Y. Li, Y. Cao, C. Wang and W. Wu, *Starch/Staerke*, 2021, **73**, 2000185.
- 54 L. Yue, W. Wang, Y. Wang, T. Du, W. Shen, H. Tang, Y. Wang and H. Yin, *Int. J. Biol. Macromol.*, 2016, **89**, 376–388.
- 55 L. Luo, Z. Zhou, J. Xue, Y. Wang, J. Zhang, X. Cai, Y. Liu and F. Yang, *Exp. Ther. Med.*, 2018, **16**, 1715–1722.
- 56 L. Luo, Y. Liu, X. Cai, Y. Wang, J. Xue, J. Zhang and F. Yang, *Saudi. J. Gastroenterol.*, 2019, **25**, 302–308.
- 57 Y. Wang, W. Huang, J. Zhang, M. Yang, Q. Qi, K. Wang, A. Li and Z. Zhao, *RSC Adv.*, 2016, **6**, 89338–89346.
- 58 H. Y. Hung and T. S. Wu, *J. Food Drug Anal.*, 2016, **24**, 221–238.
- 59 L. Dong, X. X. Liu, S. X. Wu, Y. Mei, M. J. Liu, Y. X. Dong, J. Y. Huang, Y. J. Li, Y. Huang, Y. L. Wang and S. G. Liao, *Biomed. Pharmacother.*, 2020, **130**, 110537.
- 60 Y. Zhao, Q. Wang, S. Yan, J. Zhou, L. Huang, H. Zhu, F. Ye, Y. Zhang, L. Chen, L. Chen and T. Zheng, *Front. Pharmacol.*, 2021, **12**, 659215.
- 61 C. Zhang, Y. He, Z. Chen, J. Shi, Y. Qu and J. Zhang, *J. Evidence-Based Complementary Altern. Med.*, 2019, **2019**, 9212314.
- 62 Y. Wu and C. Y. Li, *Cytotechnology*, 2025, **77**, 49.
- 63 Q. Li, K. Li, S.-S. Huang, H.-L. Zhang and Y.-P. Diao, *Asian J. Chem.*, 2014, **26**, 3574–3580.
- 64 J. Dai, S. Zhou, M. Liu, *et al.*, *Anhui Agric. Sci. Bull.*, 2015, **21**, 3.
- 65 G. Li, Y. Zhang, E. Xie, X. Yang, H. Wang, X. Wang, W. Li, Z. Song, Q. Mu, W. Zhan, Q. Wu, J. Huang, Y. Chen, Y. Zhang, F. Wang and J. Min, *Life Sci.*, 2019, **219**, 11–19.
- 66 W. Liu and H. Mo, *Chin. J. Immunol.*, 2021, **37**, 941–945.
- 67 Y. Liu, C. Sun, G. Zhang, J. Wu, L. Huang, J. Qiao and Q. Guan, *Int. J. Biol. Macromol.*, 2020, **142**, 277–287.
- 68 S. Wang, J. Yu, Y. Liu, J. Yu, Y. Ma, L. Zhou, X. Liu, L. Liu, W. Li and X. Niu, *J. Ethnopharmacol.*, 2024, **323**, 117680.
- 69 T. Chen, X. Guo, Y. Huang, W. Hao, S. Deng, G. Xu, J. Bao, Q. Xiong and W. Yang, *J. Biomater. Sci., Polym. Ed.*, 2023, **34**, 1157–1170.
- 70 L. Wang, Y. Wu, J. Li, H. Qiao and L. Di, *Int. J. Biol. Macromol.*, 2018, **120**, 529–536.
- 71 N. Li, G. Zhang, X. Zhang, Y. Liu, Y. Kong, M. Wang and X. Ren, *Int. J. Biol. Macromol.*, 2024, **261**, 129667.
- 72 N. L. Morozowich, J. L. Nichol and H. R. Allcock, *J. Polym. Sci., Part A: Polym. Chem.*, 2016, **54**, 2984–2991.
- 73 X. Tian, X. Ji, R. Zhang, X. Long, J. Lin, Y. Zhang, L. Zhan, J. Luan, G. Zhao and X. Peng, *J. Biomater. Appl.*, 2025, **39**, 487–497.
- 74 A. Zennifer, S. Manivannan, S. Sethuraman, S. G. Kumbar and D. Sundaramurthi, *Biomater. Adv.*, 2022, **134**, 112576.
- 75 G. Ye, R. Jimo, Y. Lu, Z. Kong, Y. Axi, S. Huang, Y. Xiong, L. Zhang, G. Chen, Y. Xiao, P. Li, K. Gou and R. Zeng, *Int. J. Biol. Macromol.*, 2024, **254**, 127914.
- 76 Y. Zhang, X. Han, J. Zhao, M. Gan, Y. Chen, J. Zhang, Y. He, M. Wu and H. Liu, *Biointerphases*, 2024, **19**(2), 021002.
- 77 W. Hu, Z. Wang, Y. Xiao, S. Zhang and J. Wang, *Biomater. Sci.*, 2019, **7**, 843–855.
- 78 Y. Fan, R. Hong, X. Sun, Q. Luo, H. Wei, Y. Chen, Z. Zhang, X. Zhou and J. Wan, *Int. J. Biol. Macromol.*, 2024, **258**, 128815.



- 79 H. Li, P. Yang, P. Pageni and C. Tang, *Macromol. Rapid Commun.*, 2017, **38**(14), 1700109.
- 80 C. Chen, P. Zhou, C. Huang, R. Zeng, L. Yang, Z. Han, Y. Qu and C. Zhang, *Carbohydr. Polym.*, 2021, **273**, 118557.
- 81 G. Zhong, P. Lei, P. Guo, Q. Yang, Y. Duan, J. Zhang, M. Qiu, K. Gou, C. Zhang, Y. Qu and R. Zeng, *Small*, 2024, **20**, e2309568.
- 82 L. Yang, Z. Han, C. Chen, Z. Li, S. Yu, Y. Qu and R. Zeng, *Mater. Sci. Eng., C*, 2020, **117**, 111265.
- 83 S. Zhao, J. Zhang, M. Qiu, Y. Hou, X. Li, G. Zhong, K. Gou, J. Li, C. Zhang, Y. Qu and X. Wang, *Int. J. Biol. Macromol.*, 2024, **254**, 127761.
- 84 J. Wang, L. Zhang, L. Wang, J. Tang, W. Wang, Y. Xu, Z. Li, Z. Ding, X. Jiang, K. Xi, L. Chen and Y. Gu, *Adv. Healthcare Mater.*, 2024, **13**, e2303851.
- 85 J. Shang, L. Duan, W. Zhang, Q. Zhuang, X. Ren and D. Gu, *J. Biomater. Appl.*, 2024, **38**, 943–956.
- 86 Z. Tang, N. Dan and Y. Chen, *Int. J. Biol. Macromol.*, 2024, **259**, 128389.
- 87 J. Lv, H. Ma, G. Ye, S. Jia, J. He and J. Wu, *Mater. Des.*, 2023, **226**, 111655.
- 88 N. S. Chandra, S. Gorantla, S. Priya and G. Singhvi, *Carbohydr. Polym.*, 2022, **297**, 120014.
- 89 P. Pahuja, S. Arora and P. Pawar, *Expert Opin. Drug Delivery*, 2012, **9**, 837–861.
- 90 X. Wu, X. Yang, H. Jiang, Y. Xu, T. Liu, X. Zang and H. Gong, *J. Ocul. Pharmacol. Ther.*, 2012, **28**, 369–380.
- 91 X. G. Wu, M. Xin, H. Chen, L. N. Yang and H. R. Jiang, *J. Pharm. Pharmacol.*, 2010, **62**, 1152–1157.
- 92 S. H. Chen, P. Y. Chou, Z. Y. Chen, D. C. Chuang, S. T. Hsieh and F. H. Lin, *Carbohydr. Polym.*, 2020, **250**, 116981.
- 93 R. Yang, D. Wang, H. Li, Y. He, X. Zheng, M. Yuan and M. Yuan, *Molecules*, 2019, **24**(11), 2104.
- 94 L. F. Sun, M. M. Li, Y. Chen, W. J. Lu, Q. Zhang, N. Wang, W. Y. Fang, S. Gao, S. Q. Chen and R. F. Hu, *Colloids Surf., B*, 2023, **229**, 113453.
- 95 H. Ma, Y. Axi, Y. Lu, C. Dai, S. Huang, Z. Kong, R. Jimo, H. Li, G. Chen, P. Li, L. Zhang, Y. Qu, X. Qin, R. Zeng and K. Gou, *Int. J. Biol. Macromol.*, 2024, **265**, 130780.
- 96 X. Zhang, Y. Wu, H. Gong, Y. Xiong, Y. Chen, L. Li, B. Zhi, S. Lv, T. Peng and H. Zhang, *Small*, 2024, e2400516, DOI: [10.1002/smll.202400516](https://doi.org/10.1002/smll.202400516).
- 97 X. Yue, S. Zhao, M. Qiu, J. Zhang, G. Zhong, C. Huang, X. Li, C. Zhang and Y. Qu, *Carbohydr. Polym.*, 2023, **312**, 120831.
- 98 H. Y. Zhang, K. T. Wang, Y. Zhang, Y. L. Cui and Q. Wang, *Int. J. Biol. Macromol.*, 2023, **253**, 127189.
- 99 Z. Ma, X. Yang, J. Ma, J. Lv, J. He, D. Jia, Y. Qu, G. Chen, H. Yan and R. Zeng, *Colloids Surf., B*, 2021, **208**, 112066.
- 100 X. Yang, M. Jia, Z. Li, Z. Ma, J. Lv, D. Jia, D. He, R. Zeng, G. Luo and Y. Yu, *Int. J. Biol. Macromol.*, 2022, **215**, 550–559.
- 101 P. Zhou, S. Zhao, C. Huang, Y. Qu and C. Zhang, *Int. J. Biol. Macromol.*, 2022, **205**, 511–519.
- 102 L. Hu, Z. Liao, Q. Hu, K. G. Maffucci and Y. Qu, *Int. J. Biol. Macromol.*, 2018, **117**, 928–936.
- 103 T. Wu, X. Hou, J. Li, H. Ruan, L. Pei, T. Guo, Z. Wang, T. Ci, S. Ruan, Y. He, Z. He, N. Feng and Y. Zhang, *ACS Nano*, 2021, **15**, 20087–20104.

